

The Measurement System for Particle Size on Surface of Hard Disk Drive based on Experimental Light Scattering of BRDF Simulation

Mongkol Wannaprapa¹,

Narongpun Rungcharoen², and Wanchai Pijitrojana³, Non-members

ABSTRACT

This work aims to obtain the perfectly measurement system for 200-600 nanometer of particle size, type of SiO₂ on surface of Lubricant (n_D^{20}) recording media of hard disk drive, at 448 and 635 nm of incident wavelength. This system uses an incident and reflective angles equally, 89°, based on the principle of Mie scattering theory. Moreover, the system is applied to compare an intensity value of scattered light between of BRDF_{part} simulation model and of experiment result of David W. Hahn light scattering. For the conclusion, this system could measure the particle sizes and types accurately and efficiently.

Keywords: Scattering Intensity, BRDF_{part} Simulation Model, Mie Scattering Theory, Particle Sizes, Particle Types

1. INTRODUCTION

Although a hard disk drive has been nowadays developed to smaller size, it is low efficiency and causes damage to the inner components of hard disk drive because of contaminated small particle during production process. As a result, ones are interested in studying to use the scattering technologies for analyzing the sizes and types of particles, which are indicated at level of nanometer (nm) scale.

For example, Yuzo MORI and his team studied on "A New Apparatus for Measuring Particle Sizes of the Order of Nanometer". They innovated the measurement system on Silicon (Si) wafer surface of refractive index at 1.5 within particle sizes of 1-30 nm, including five types of Ag, Au, SiC, Al₂O₃ and SiO₂ which respectively contain the refractive index of particle at 0.23, 1.46, 2.46, 1.76 and 1.45 [1], with the incident light at 448 nm of wavelength.

The result based on Rayleigh Scattering Theory [8], the average measurement of scattering intensity

for five particle types, comparing with 1-30 nm of particle size which is consequent to particle types and sizes. The result and diagram of the measurement system are shown in fig.1 and fig.2.

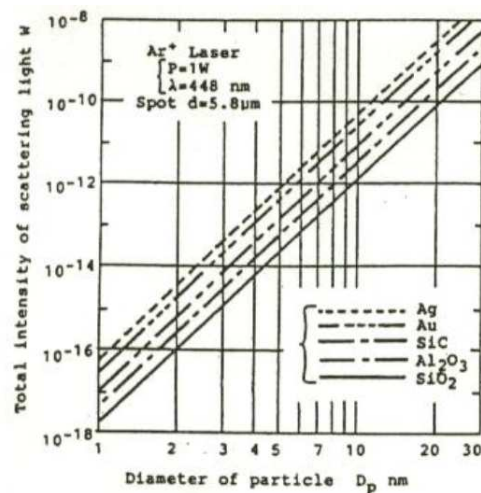


Fig.1: Yuzo MORIs experimental result based on Rayleigh scattering theory [6]

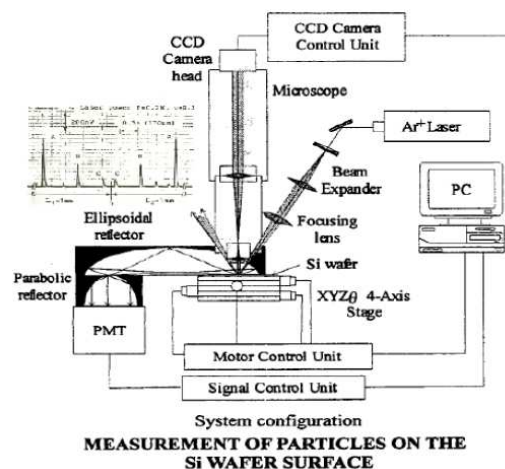


Fig.2: Yuzo MORIs measurement of particles on the Si wafer surface [7]

Manuscript received on August 1, 2010 ; revised on January 11, 2011.

^{1,2,3} The authors are with Department of Electrical Engineering, Faculty of Engineering, Thammasat University Rangsit CampusKlong Luang, Pathumthani 12120, Thailand., E-mail:w_mongkol@hotmail.com, narongpun@gmail.com and pwanchai@engr.tu.ac.th

Besides, David W. Hahn [5] had researched on light scattering based on Mie Scattering Theory [3]. His experiment used scattered light at 1.7 micrometer of spherical particle with refractive index of 1.4 and 0° - 180° of incident angles vertically at particular area with wavelength of 532 nm and 90° of θ_i angle, as shown in fig. 3.

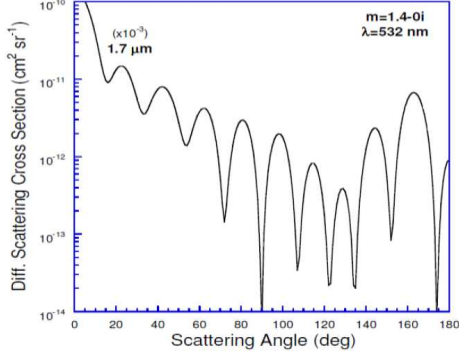


Fig.3: David W. Hahns light scattering at 1.7 m base on Mie scattering theory [5]

In this work, we use the principle of Bidirectional Reflectance Distribution Function (BRDF) [4] to model and design the system using Modeled Integrated Scattering Tool program (MIST) [11]. In order to study the characteristics of scattered light from particle on surfaces, the BRDF_{part} simulation model based on Rayleigh and Mie scattering theories are specified patterns. Then, the results of the simulations are compared to the experimental result of Yuzo MORI [6] using Rayleigh scattering theory and David W. Hahn [5] using Mie scattering theory. It is confirmed that the simulation model and designing of the system are well-defined and lead to implementation of the real measurement system for both size and type of particle, size ranged from 200 to 600 nm and type of SiO₂, on surface of Lubricant (n_D²⁰) recording media of hard disk drive [2].

2. PRINCIPLES AND THEORIES

2.1 Scattering Principle

The light scattering is the alteration of the direction and intensity of a light beam that strikes an object, the alteration is due to the combined effects of reflection, refraction, and diffraction [3] as shown in fig. 4.

This phenomenon is based on Rayleigh and Mie scattering theories, which α value classifies the type of scattered light. The formula is defined by the particle size and reciprocal wavelength of the incident light [1].

$$\alpha = \frac{\pi D}{\lambda} \quad (1)$$

D is the diameter of particle

λ is the wavelength of incident light

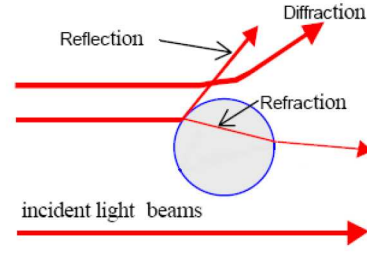


Fig.4: Phenomenon of scattering particle [3]

Where $\alpha \ll 1$ [Based on Rayleigh Scattering Theory]
 $\alpha \gg 1$ [Based on Mie Scattering Theory]

2.2 Rayleigh Scattering Theory

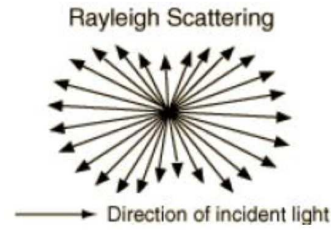


Fig.5: Rayleigh scattering [9]

According to fig. 5, the incident light on small particle with $\alpha \ll 1$ value, which the intensity of scattered light equal to the intensity of light scattering occurs all around area, which is called Rayleigh scattering theory as following formula (2).

$$I_{Ray} = I_0 \frac{1 + \cos^2 \theta}{2R^2} \left(\frac{2\pi}{\lambda} \right) \left(\frac{D}{2} \right)^6 \left(\frac{n^2 - 1}{n^2 + 2} \right)^2 \quad (2)$$

I_0 is incident light intensity

θ is the scattering angle

R is distance of scattered

n is refractive index of particle

2.3 Mie Scattering Theory

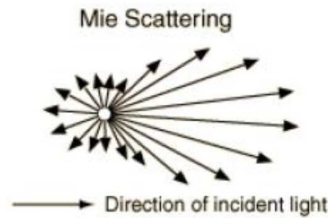


Fig.6: Mie scattering theory [9]

Refer to fig. 6, the incident light on particle with $\alpha \gg 1$ value, which the intensity of scattered light

has high scattering intensity in the inverse direction of incident light, which is called Mie scattering theory as following formula (3).

$$I_{Mie} = I_o \frac{1}{2R^2} \left(\frac{2\pi}{\lambda} \right)^4 \left(\frac{D}{2} \right)^6 (i_{\perp} + i_{\parallel}) \quad (3)$$

Where i_{\perp} , i_{\parallel} are the intensity function of computation from the infinite series.

2.4 Principle of Bidirectional Reflection Distribution Function (BRDF)

BRDF is property of the incident light on material obtained from optical interaction with three characterizations; Reflected light, Transmitted light, and Absorbed light, which is called Energy conservation [10], as shown in fig. 7.

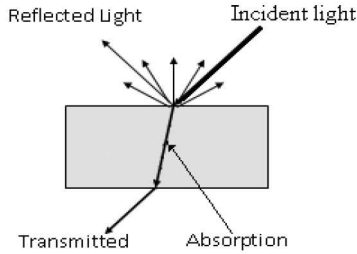


Fig.7: BRDFs light reaction [10]

$$\text{Incident light} = \text{Reflected light} + \text{Transmitted light} + \text{Absorbed light}$$

BRDF is considered by the ratio of reflected light signal and incident light signal, as referred to formula (4).

$$BRDF = \frac{\text{OutputSignal}}{\text{InputSignal}} = \frac{L_r}{E_i} \quad (4)$$

L_r is quantity of light reflected in direction ω_r

E_i is quantity of light arriving in direction ω_i

ω_i is incoming light direction

ω_r is outgoing reflected direction

Due to formula (4), it can be considered by the incident light angle and reflected light angle as following formula (5).

$$BRDF(\theta_i, \phi_i, \theta_r, \phi_r) = \frac{dL_r(\theta_i, \phi_i, \theta_r)}{dE_i(\theta_i, \phi_i)} \quad (5)$$

θ_i is the zenith angle of incident light

ϕ_i is the azimuth angle of incident light

θ_r is the zenith angle of reflected light

ϕ_r is the azimuth angle of reflected light

To obtain the incident light angle and the reflected light angle under BRDF principle, it can be described as geometric structure as shown in fig.8.

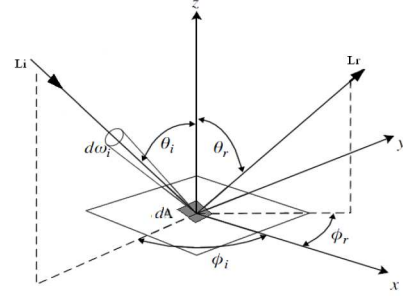


Fig.8: Geometric structure on BRDF surface

Refer to fig. 8, the incident light angle of L_i is correlated to Solid Angle : $d\omega$ which contains the incident light angle of θ_i and Azimuth angle of incident light angle ϕ_i on xy plane in an area of dA_i . If so, the reflected light angle of direction L_r is correlated to solid angle θ_r , ϕ_r on xy plane. Thus, BRDF can show geometric structure on half sphere as referred to fig. 9.

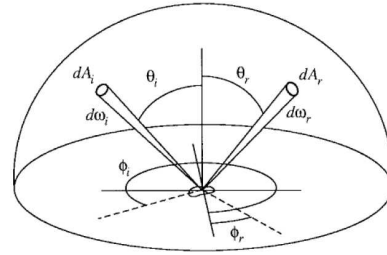


Fig.9: BRDFs geometric structure on half sphere

Due to the spherical solid angle tariff (fig. 8), $d\omega$ and dE_i triangle defined as follows:

$$d\omega = (\text{height})(\text{width}) = (d\theta)(\sin\theta d\phi) = \sin\theta d\theta d\phi \quad (6)$$

$$\text{and} \quad dE_i = L_i \cos\theta_i d\omega_i \quad (7)$$

Thus, formulas (6) and (7) are defined small area on spherical surface, as shown in fig 10, of solid angle in BRDF direction between reflected light angle and incident light angle.

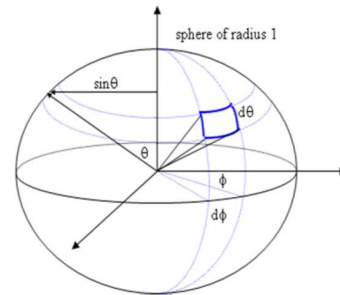


Fig.10: Tariff of spherical solid angle

Therefore, formulas (4) and (5) of BRDF take place by formulas (6) and (7) on incident angle of light as formula (8).

$$BRDF(\theta_i, \phi_i, \theta_r, \phi_r) = \frac{L_r}{L_i \cos \theta_i d\omega_i} \quad (8)$$

Refer to above principle of BRDF, BRDF_{part} simulation model on MIST program will be analyzed particle on surface as following (9).

$$BRDF_{part} = \frac{1}{\cos \theta_r \cos \theta_i} \frac{NF}{A} \times |q_{ij}^{part}| \cdot \hat{e}^2 \left(\frac{2\pi}{\lambda} \right)^4 \left(\frac{D}{1} \right)^6 \left(\frac{n_{sph}^2 - 1}{n_{sph}^2 + 2} \right)^2 \quad (9)$$

N/A is density of scatters within the illuminated area

F is structure factor that depends upon the correlation between different scattering centers.

n_{sph} is refractive index of particle

\hat{e} is a unit vector parallel to the incident electric field.

q_{ij} is Jones scattering matrix value

3. RESULTS AND DISCUSSIONS

3.1 Results of BRDF_{part} Simulation Model Comparing between Incident Angle and Reflected Angle for Suitable Scattering Intensity

To create BRDF_{part} simulation model by defining the incident angle and reflected angle, the conditions are the laser source with 532 nm wavelength and the incident light direction L_i that affects the reflected light direction L_r at θ_i and θ_r angles as shown in fig. 11. BRDF_{part} value will be defined as formula (9) by the incident light on particle with the size of 10 and 100 micrometer, the spherical shape of Polystyrene latex (PSL) at refractive index of 1.59 [1] on Lubricant (n_D^{20}) recording media of hard disk drive as shown in fig. 11.

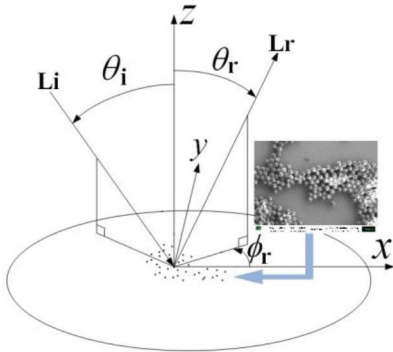


Fig.11: BRDFs geometric structure on PSL particle, surface of Lubricant recording media of hard disk drive

As the results of BRDF_{part} simulation model comparing between incident and reflected angles at 1° ,

45° and 89° under 10 and 100 micrometer, both incident and reflected angles at 89° contain the highest BRDF_{part} value. We could conclude that the angle for accurate and suitable measuring at 10 and 100 micrometer of particle size is 89° angle as shown in fig. 12 and 13.

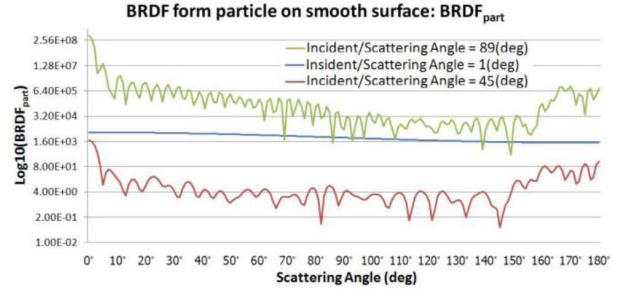


Fig.12: Comparison between incident angle at (1° , 45° , 89°) and reflective angle at (1° , 45° , 89°) on 10 micrometer of particle

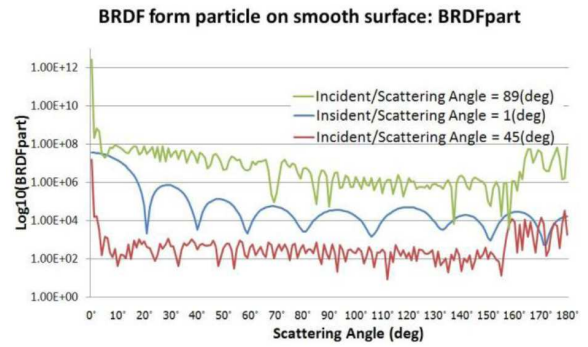


Fig.13: Comparison between incident angle at (1° , 45° , 89°) and reflective angle at (1° , 45° , 89°) on 100 micrometer of particle

From the incident and reflected angle at 89° , we use it to compare the results of this paper to BRDF simulation of Rayleigh and Mie scattering theory.

3.2 Yuzo MORIs Result compare with the Results of BRDF_{part} Simulation Model to based on Rayleigh Scattering Theory

Comparison between Yuzo MORIs experimental result and the results of BRDF_{part} simulation model based on Rayleigh scattering theory are used to define the number of angles measuring scattering intensity at 360 points, incident and reflected angle at 89° under the same as other conditions and variables, and also is used to find the average scattering intensities. The conclusion results of simulation correlated with Yuzo MORIs real experiment. Because the increasing ratio of light scattering intensity is associated to the increasing particle size in ranged from 1 to 30 nm which the slope and linear with all five types are

shown in fig. 14. Thus, the results of this comparison relates to the principle of $BRDF_{part}$ simulation model.

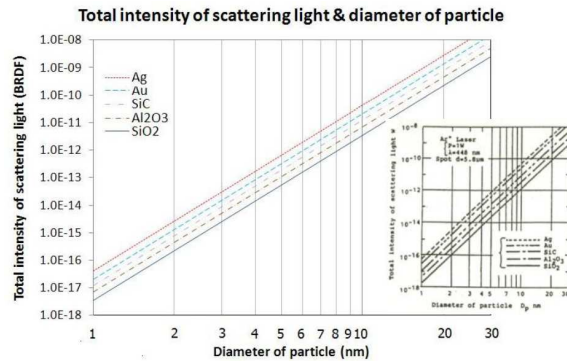


Fig.14: Results of $BRDF_{part}$ simulation model at 89° incident and reflective angle under conditions of Yuzo MORIs experiment

According to above results, the number of particle sizes has increased from 1-30 nm to 1-600 nm on surface of Ag, Au, SiC, Al_2O_3 and SiO_2 types in order to consider the correlation between sizes and average of light scattering intensities as shown in fig. 15.

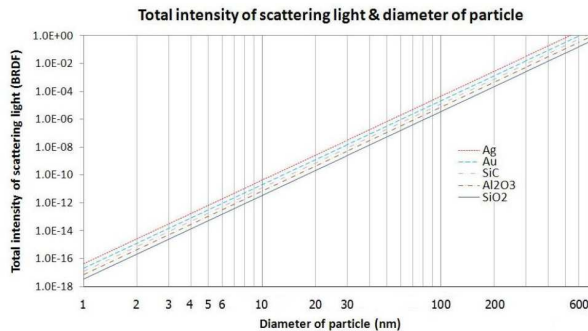


Fig.15: Results of $BRDF_{part}$ simulation model at 1600 nm on Si wafer surface

Fig. 15 shows the relationship between the particle sizes continuously increasing in ranged from 100 to 600 nm and the intensity of scattered light linearly increasing. Thus, we are able to apply $BRDF_{part}$ simulation model to define the average of light scattering from 100 to 600 nm particle sizes on surfaces of Ag, Au, SiC, Al_2O_3 and SiO_2 types as shown in fig. 16.

From the experiment, we measure three particle types of TiO_2 , Al_2O_3 and SiO_2 . Si wafer is used in the experiment instead of Lubricant recording media of hard disk drive in order to observe the linearity of scattering intensity.

Particle sizes in ranged from 100 to 600 nm and type of particle: TiO_2 , Al_2O_3 and SiO_2 relate to the intensity of scattered light as shown in fig. 17. Obviously, the intensity of scattering is directly changed with the particle sizes in the pattern of linearity.

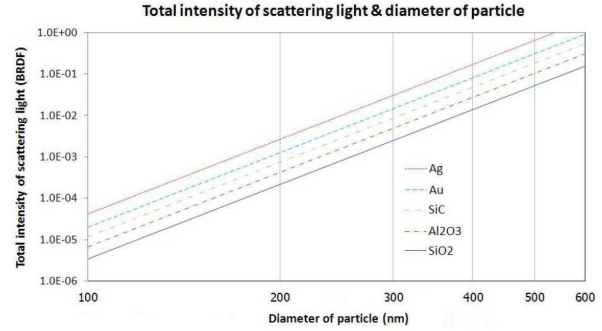


Fig.16: Result of $BRDF_{part}$ simulation model on surfaces of Ag, Au, SiC, Al_2O_3 and SiO_2 particle ranged from 100 - 600 nm on Si wafer surface

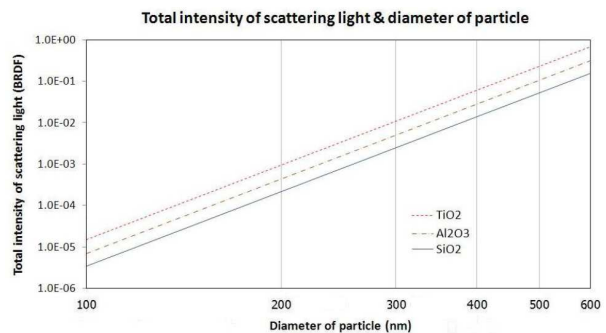


Fig.17: Results of $BRDF_{part}$ simulation model with TiO_2 , Al_2O_3 and SiO_2 particle at 100600 nm on Lubricant recording media of hard disk drive

3.3 David W. Hahns Result compare with Results of $BRDF_{part}$ Simulation Model based on Mie Scattering Theory

In this case, it is similar to the results in section 3.2. The comparison between David W. Hahns experimental result and the results of $BRDF_{part}$ simulation model based on Mie scattering theory is used to define the number of angles for measuring scattering intensity at 180 points. This results of simulation correlates with the result of David W. Hahns experiment. Consequently, the results of comparison relate to the principle of $BRDF_{part}$ simulation model theory as shown in fig. 18.

3.4 Results of $BRDF_{part}$ Simulation Model base on Rayleigh and Mie Scattering Theories

According to fig. 19 and 20, the results of Rayleigh and Mie scattering theories are different. We can combine these two scattering theories to consider the correlation of sizes ranged from 1 - 100 nm and from 200 - 600 nm.

The first range of sizes of particle is 1-100 nm with $\alpha \ll 1$ value based on Rayleigh scattering theory as shown in table 1. Firstly, the smallest particle size, 1 nm. , shown as the first inner-circle gives the low-

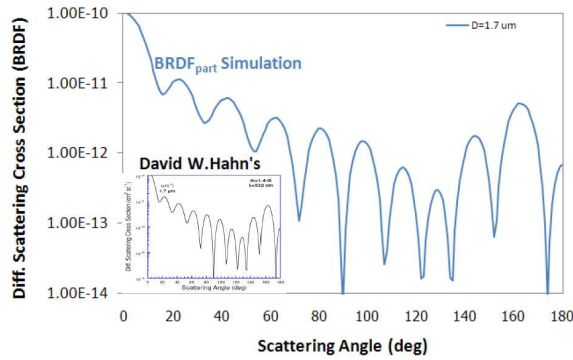


Fig.18: $BRDF_{part}$ simulation model on particle at $1.7 \mu m$ ($m = 1.4-0i$) with wavelength at 532 nm comparison with David W. Hahns

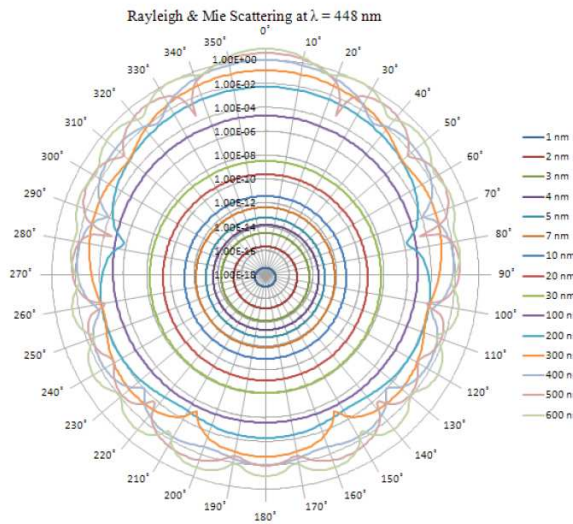


Fig.19: Rayleigh and Mie scattering theories with wavelength at 448 nm on SiO_2 particle sizing $1-600 \text{ nm}$ on (n_D^{20}) surface

est intensity of scattered light. Secondly, the particle size, 100 nm , shown as the ninth circle gives the highest intensity of scattered light. Finally, the other particle sizes give the proportion of intensity of scattered light. The second range of sizes of particle is $200-600 \text{ nm}$ with $\alpha \gg 1$ value based on Mie scattering theory. Similarly, the increasing of scattered light intensity directly change according to the increasing of particle sizes. The scattered light intensities of the particle sizes ranged from $200-600 \text{ nm}$ are higher than of the particle sizes ranged from $1-100 \text{ nm}$.

Table 1 shows, the calculation of parameters of α values according to the particle size of $1-600 \text{ nm}$ with λ are 448 and 635 nm . For instance, $\alpha = (3.14) (7 \times 10^{-9}) / (448 \times 10^{-9}) = 0.049$ ($\alpha \ll 1$) shows that scattering theory is based on Rayleigh. Similarly, $\alpha = (3.14) (400 \times 10^{-9}) / (635 \times 10^{-9}) = 1.978$ ($\alpha \gg 1$) shows that scattering theory is based on Mie. From the calculations, we obtain the suitable patterns of

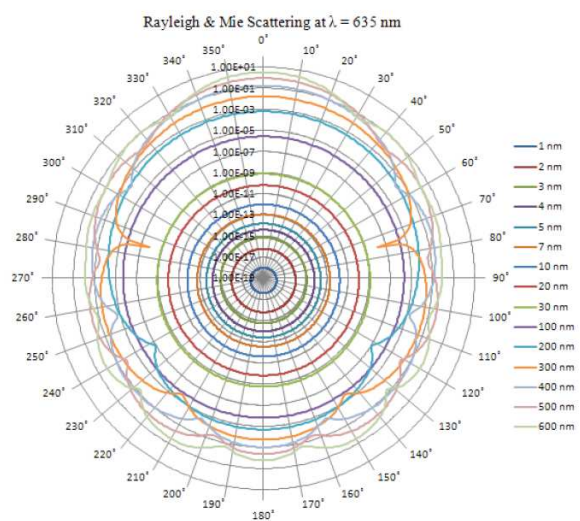


Fig.20: Rayleigh and Mie scattering theories at 635 nm wavelength on the particle type of SiO_2 , sizing $1-600 \text{ nm}$ on (n_D^{20}) surface

Table 1: α value presents the relation between D particle sizing $1-600 \text{ nm}$ and $448, 635 \text{ nm}$ wavelengths

$\alpha = \pi D / \lambda$				
Dimeter (D)	Parameter (α)	Wavelength ($\lambda = 448 \text{ nm}$)	Wavelength ($\lambda = 635 \text{ nm}$)	
1 nm	$(\alpha \ll 1)$	0.007	0.005	Rayleigh Scat.
2 nm		0.014	0.010	
3 nm		0.021	0.015	
4 nm		0.028	0.020	
5 nm		0.035	0.025	
7 nm		0.049	0.035	
10 nm		0.070	0.049	
20 nm		0.140	0.099	
30 nm		0.210	0.148	
100 nm		0.701	0.494	
200 nm	$(\alpha \gg 1)$	1.402	1.000	Mie Scat.
300 nm		2.103	1.483	
400 nm		2.804	1.978	
500 nm		3.504	2.472	
600 nm		4.205	2.967	

scattered light intensities.

Clearly, fig. 21-22 and 23-24 show separately for Rayleigh and Mie scattering theories with wavelengths at 448 nm and 635 nm .

Firstly, $BRDF_{part}$ simulation model is under condition of $\alpha \ll 1$ in table 1 on particle size of $1-100 \text{ nm}$ at $448, 635 \text{ nm}$ wavelengths as shown in fig. 21 and 22. The innermost circle: particle size of 1 nm at two wavelengths gives the lowest light scattering intensity and the outermost circle: particle size of 100 nm at two wavelengths gives the highest light scattering intensity respectively. Clearly, the results obtained agree with Rayleigh scattering theory. Because the pattern of these light scattering intensities are the same pattern of Rayleigh scattering theory, i.e. there are light scattering intensities all directions equally.

Secondly, $BRDF_{part}$ simulation mode is under condition of $\alpha \gg 1$ in table 1 on particle size of $200-600 \text{ nm}$ at $448, 635 \text{ nm}$ wavelengths as shown in fig. 23 and 24. Similarly, both of the particle size of 200

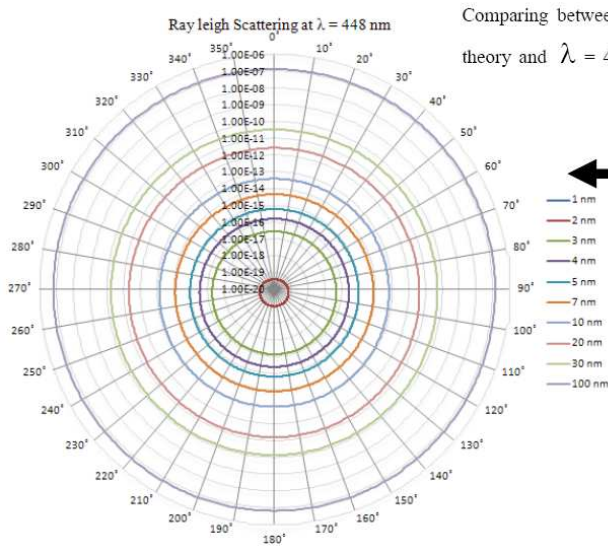


Fig.21: Rayleigh scattering theory at 448 nm on SiO_2 particle sizing of 1-100 nm on (n_D^{20}) surface

Comparing between Rayleigh scattering theory and $\lambda = 448 \text{ nm}$, $\lambda = 635 \text{ nm}$

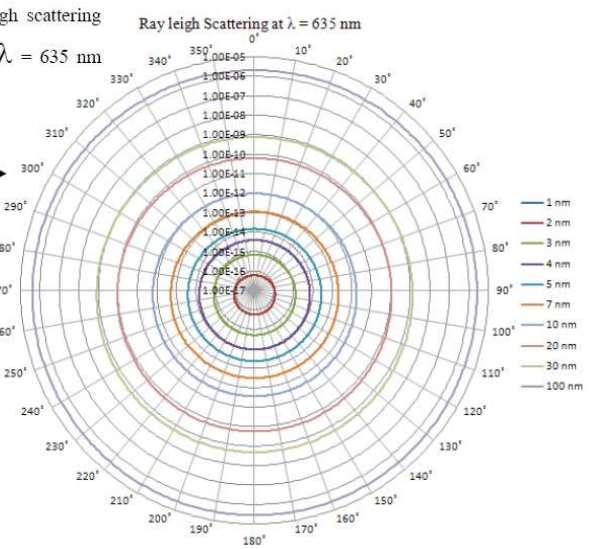


Fig. 22: Rayleigh scattering theory at 635 nm on SiO_2 particle sizing of 1-100 nm on (n_D^{20}) surface

Comparing between Rayleigh and Mie scattering theories at $\lambda = 448 \text{ nm}$

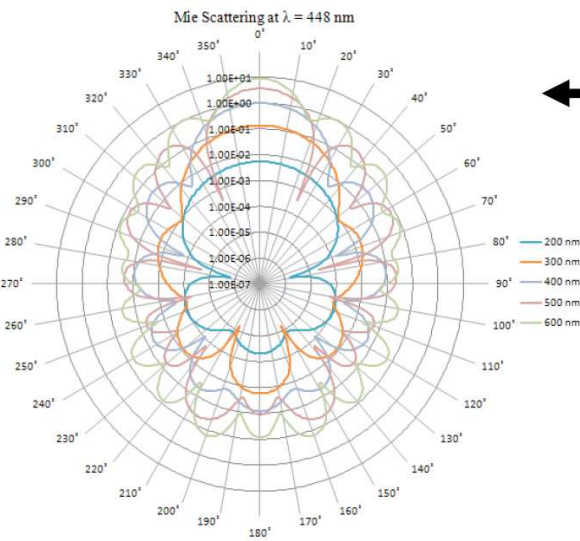


Fig.23: Mie scattering theory at 448 nm on SiO_2 particle sizing of 200-600 nm on (n_D^{20}) surface

Comparing between Mie scattering theory and $\lambda = 448 \text{ nm}$, $\lambda = 635 \text{ nm}$

Comparing between Rayleigh and Mie scattering theories at $\lambda = 635 \text{ nm}$

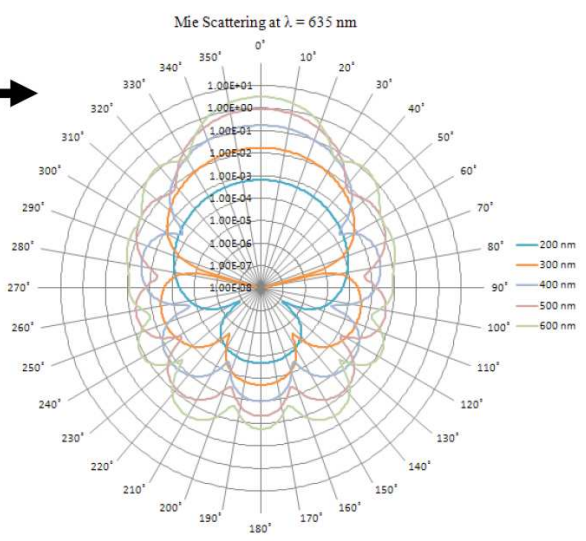


Fig. 24: Mie scattering theory at 635 nm on SiO_2 particle sizing of 200-600 nm on (n_D^{20}) surface

and 600 nm, at two wavelengths, give the increasing of scattered light intensity directly changed according to the increasing of particle sizes and give the same pattern of Mie scattering theory, i.e. the light scattering intensities are the highest in the opposite direction to the incident light. Clearly, the results obtained agree with Mie scattering theory.

Finally, This BRDF_{part} simulation model is under the same conditions and factors. For instance, the incident and reflected angle are equal to 89° with

SiO_2 particle at refractive index of 1.45 on Lubricant recording media surface of hard disk drive at the same refractive index of 1.5. Therefore, this leads to the conclusion that BRDF_{part} simulation model can be used to design and construct the system to measure sizes and types of particle on Lubricant recording media surface base on Rayleigh or Mie scattering theory. For this paper, the particle size is defined between 200-600 nm at parameter equal to $\alpha \gg 1$ according to Mie scattering theory.

4. CONCLUSION

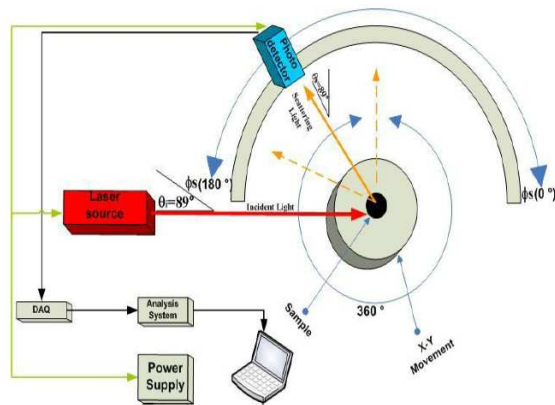


Fig.25: The measurement system for spherical particle on smooth surface based on the principle of Mie scattering theory

According to the principle of scattering theory and the results of BRDF simulation model of this work, we can confirm the results of the BRDF compared between Yuzo MORI's Result and David W. Hahn's Result are properly and appropriately. We can conclude that the BRDF simulation can be used in order to measure for 200-600 nm, SiO₂ particle on Lubricant recording media surface based on Mie scattering theory. Besides, the BRDF can measure other particles, other surfaces, based on Mie or Rayleigh scattering theory. In the figure 25 shown, the design of measurement system is implemented and tested based on Mie scattering theory. The system consists of the photo detector can be moved from 0° to 180° angles and detects the intensities of light scattering. Moreover, the suitable angle of incident and reflected light is 89° angle and the samples are moveable and controllable automatically. The signals of the system are analyzed by using computer and software. Besides, the system can be developed to measure other particle sizes and types in industry of hard disk drive.

5. ACKNOWLEDGMENT

The author would like to thank the National Electronics and Computer Technology Center of Thailand and I/U CRC in HDD advanced manufacturing for financial support

References

- [1] R. Xu, "Particle characterization light scattering methods," in KLUWER ACADEMIC PUBLISHERS, ISBN: 0-792-36300-0, (2002).
- [2] <http://books.google.com/books?id=GpAO5dGXN60C&pg=PA125&lpg=PA125&dq=lubricant+refractive+index&source>.
- [3] P. A. Webb, "A primer on particle sizing by static laser light scattering," Micromeritics technical workshop series (2000).
- [4] T. A. Germer, "Angular dependence and polarization of out-of-plane optical scattering from particulate contamination subsurface defects and surface micro roughness," *SPIE* 3275, 8798-8805, (1997).
- [5] D. W. Hahn, "Light Scattering Theory," Department of Mechanical and Aerospace Engineering (2008).
- [6] Y. Mori, H. An, K. Endo, K. Yamauchi and T. Ied "A new apparatus for measuring particle sizes of the order of nanometer," *J. JSPE*, Sept 1991.
- [7] S. SASAKI, H. AN, Y. MORI, T. KATAOKA, K. ENDO "Evaluation of particle on a Si wafer before and after cleaning using a new laser particle counter," *IEEE*, 317-320, 26-28 Sept.
- [8] <http://hyperphysics.phy-astr.edu/hbase/atmos/blusky.html>. 28-Feb-2006.
- [9] http://commons.wikimedia.org/wiki/Image:Mie_scattering.svg.
- [10] C. Wym "An introduction to BRDF-based lighting", NVIDIA Corporation.
- [11] Thomas A. Germer "Modeled integrated scatter tool (MIST)", Available free of charge from NIST: <http://physics.nist.gov/scatmech> (2006).



Mongkol Wannaprapa received his Bachelor of Engineering (B. Eng) and Master of Engineering (M.Eng) in electrical engineering from the King's Mongkut Institute of Technology Ladkrabang (KMUTL), Thailand.



Narongpun Rungcharoen received his Bachelor of Engineering (B. Eng) in electrical engineering from the King's Mongkut University of Technology Thonburi (KMUTT), Thailand. He also received the Master of Engineering (M.Eng) in electrical engineering from Thammasat University (TU), Thailand.



Wanchai Pijitrojana received the B.Eng. degree in Telecommunication Engineering from King's Mongkut Institute of Technology, Ladkrabang, Bangkok, Thailand. He also received the M.S. degree in both, Computer Technology and Nonlinear Optics (Electrophysics) from Asian Institute of Technology, Bangkok, Thailand and the University of Southern California, California, U.S.A., respectively, and the Ph.D. degree in Optoelectronics from King's College, University of London, London, England. He is currently a lecturer in the EE Department, Thammasat University, Bangkok, Thailand. His current research interests are Optical Interconnection systems, Optical Design, Optics, Nonlinear Optics, Physical Optics, PBG, and Mathematics applied to Optics.